Supplementary Information

S1. Theory

There are various approaches to incorporate the nuclear quantum effect into calculation results, such as methods based on multicomponent scheme[1-6], path integral molecular dynamics (PIMD) method[7-10], and some other methods based on the vibrational Schrödinger equation[11-16].

□□□In the multicomponent density functional theory (MC_DFT)[2], based on multicomponent scheme, the total Hamiltonian is expressed as

$$\begin{aligned} H_{tot} = &-\sum_{i}^{N_e}\frac{1}{2}\nabla_i^2 - \sum_{i}^{N_e}\sum_{A}^{M}\frac{Z_A}{r_{iA}} + \sum_{i>j}^{N_e}\frac{1}{r_{ij}} - \sum_{p}^{N_p}\frac{1}{2M_p}\nabla_p^2 \\ &+\sum_{p}^{N_p}\sum_{A}^{M}\frac{Z_pZ_A}{r_{pA}} + \sum_{p>q}^{N_p}\frac{Z_pZ_q}{r_{pq}} - \sum_{i}^{N_e}\sum_{p}^{N_p}\frac{Z_p}{r_{ip}} + \sum_{A>B}^{M}\frac{Z_AZ_B}{R_{AB}} \end{aligned}, \qquad (1)$$

where *i* and j refer to electrons, *A* and *B* to the classical nuclei, *p* and *q* to the quantum nuclei. Z_A represents the charge of *A*th nuclei, and M_p is the mass of *p*th quantum nuclei. The first to third terms in Eq. (1) are common terms with the conventional DFT. The fourth to sixth terms are additional terms to quantum nuclear terms. The seventh term is Coulomb term between electron and quantum nucleus, and last term is the classical nucleus-nucleus repulsion. The corresponding Kohn-Sham operators for N_e-electrons and N_p-quantum nuclei are expressed as

$$f_\mathrm{e} = h_\mathrm{e} + \sum_{e}^{N_\mathrm{e}} J_e - \sum_{p}^{N_\mathrm{p}} J_p + V_{\mathrm{XC(e\text{-}e)}} + V_{\mathrm{C(e\text{-}p)}} , \tag{2}$$

$$f_\mathrm{p} = h_\mathrm{p} + \sum_{p}^{N_\mathrm{p}} J_p - \sum_{e}^{N_\mathrm{e}} J_e + V_{\mathrm{XC(p\text{-}p)}} + V_{\mathrm{C(e\text{-}p)}} , \tag{3}$$

where h and J are one particle operator and Coulomb operator, respectively, and $V_{\mathrm{XC(e\text{-}e)}}$ is electron-electron exchange-correlation term[2]. In this study, we have ignored electron-nucleus and nucleus-nucleus correlation terms, $V_{\mathrm{C(e\text{-}p)}}$ and $V_{\mathrm{XC(p\text{-}p)}}$, due to its small contribution[4].

Typical methods to address nuclear quantum effects, such as the path integral molecular dynamics, are based on Born-Oppenheimer approximation. In these methods, the nuclear quantum effects are evaluated on the potential energy surface that is obtained by electronic quantum mechanical calculation such as the conventional DFT calculation. In contrast, MC_DFT is based on the multicomponent fashion, and the quantum states of both electrons and hydrogen nuclei are simultaneously obtained. While the electronic state and the corresponding energy are unchanged by isotopic substitution in conventional DFT, MC_DFT provides the different electronic state and energy for each isotopologue, which is corrected by the nuclear quantum effect of hydrogen.

S2. Mulliken population analysis of 1 and 3-unit models

To find out why PEC was changed by π-π stacking, we would like to focus on the charge of each subunit. Table S1 shows the partial summation of Mulliken charge in each subunit (SU) and H-bonding three atoms [O…H…O] defined by Figure S2. We only discuss the case of H-TTF at 50 K, since the behavior of the charge change is similar in all of the reference structures. When the hydrogen atom is located at the center of H-bond (δ_{OH}=0.00), each subunit and H-bonding [O…H…O] part have charges of +0.5 and –1.0 in both of the 1- and 3-unit models, which is in good agreement with the results of the bond-length analyses[17,18]. The charge of H-bonding [O…H…O] part did not drastically change in both of the 1- and 3-unit models. When the hydrogen atom transferred toward SU1 from the center, charge of SU1 goes down to +0.2, and charge of SU2 goes up to +0.8 in 1-unit model. On the other hand, in the 3-unit model, change of charge in SU3 and SU4 by the hydrogen transfer is only ~0.03

when hydrogen moved to 0.25 Å. We can also see the charge of SU1, SU2, SU5, and SU6 are also changed by the hydrogen transfer. This means that the change of charge in 1-unit model is compensated by the nearest neighboring H-TTF via π-π stacking. The drastic difference of the energy barriers of 1- and 3-unit models would be attributed to such inter-unit charge compensation.

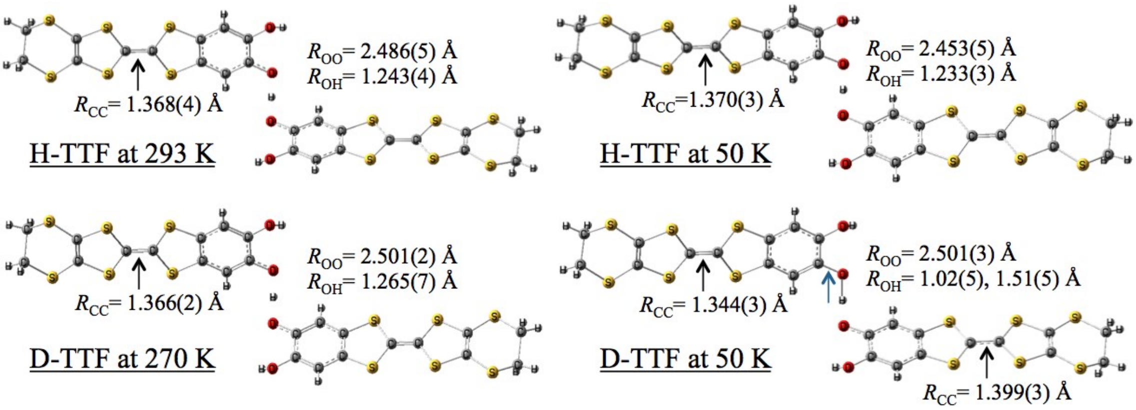

Figure S1. X-ray structures of H(D)-TTF in the 1-unit model. All the atoms including the hydrogen atoms were experimentally determined by synchrotron X-ray crystal analysis[17,18]. Note that the terminal ethylene groups in the TTF skeletons are disordered at 293 K in H-TTF and at 270 K in D-TTF, and thus, in the present calculations, we used the coordinates of these atoms with smaller temperature factors.

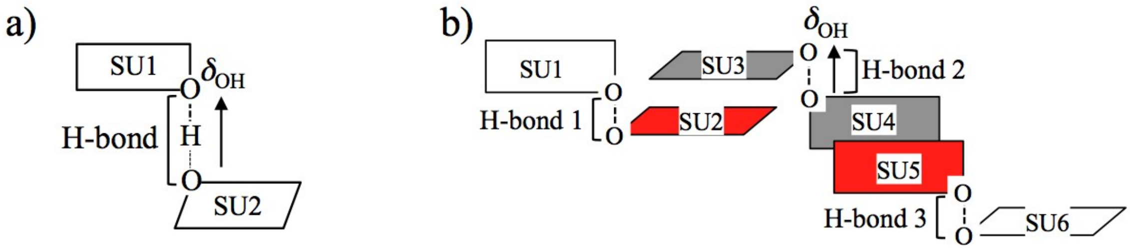

Figure S2. Definition of subunits (SUs) and H-bonding moieties in a) 1-unit model and b) 3-unit models.

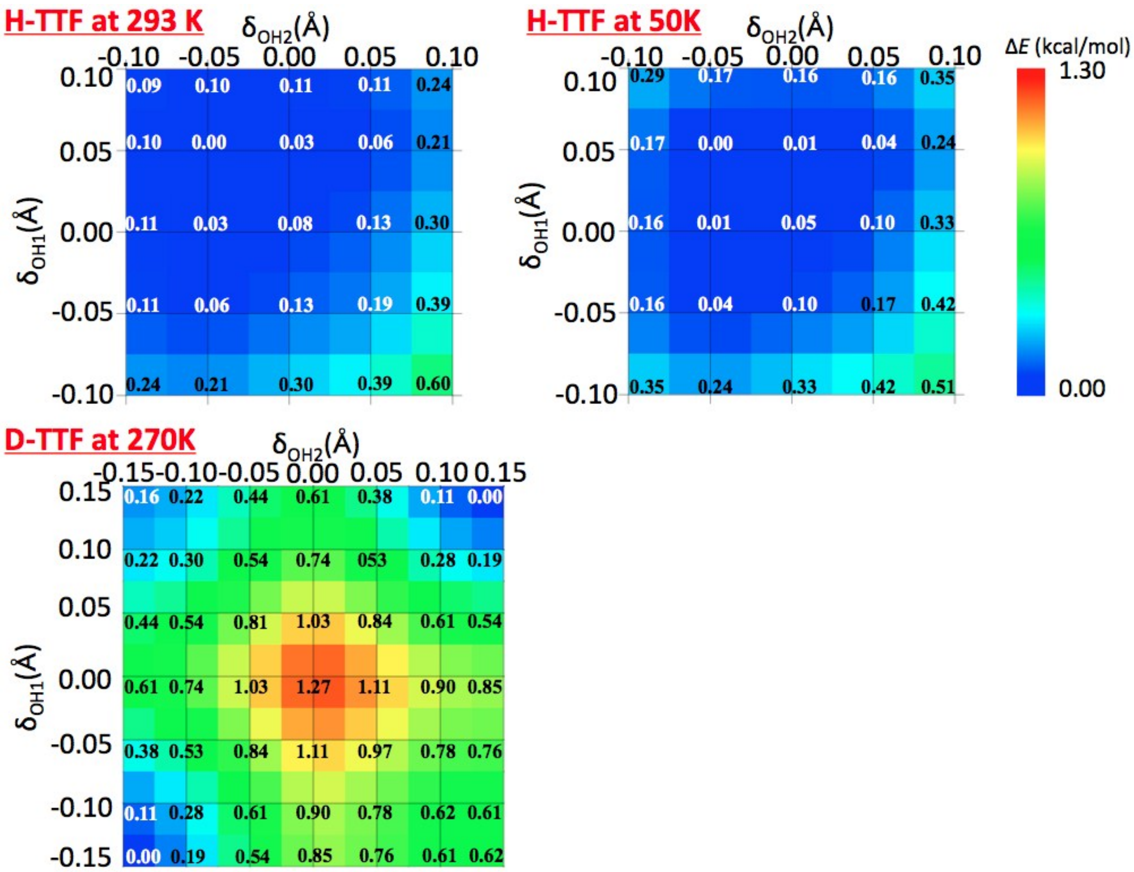

H-TTF at 293 K

δ_{OH1}(Å) \ δ_{OH2}(Å)	-0.10	-0.05	0.00	0.05	0.10
0.10	0.09	0.10	0.11	0.11	0.24
0.05	0.10	0.00	0.03	0.06	0.21
0.00	0.11	0.03	0.08	0.13	0.30
-0.05	0.11	0.06	0.13	0.19	0.39
-0.10	0.24	0.21	0.30	0.39	0.60

H-TTF at 50K

δ_{OH1}(Å) \ δ_{OH2}(Å)	-0.10	-0.05	0.00	0.05	0.10
0.10	0.29	0.17	0.16	0.16	0.35
0.05	0.17	0.00	0.01	0.04	0.24
0.00	0.16	0.01	0.05	0.10	0.33
-0.05	0.16	0.04	0.10	0.17	0.42
-0.10	0.35	0.24	0.33	0.42	0.51

D-TTF at 270K

δ_{OH1}(Å) \ δ_{OH2}(Å)	-0.15	-0.10	-0.05	0.00	0.05	0.10	0.15
0.15	0.16	0.22	0.44	0.61	0.38	0.11	0.00
0.10	0.22	0.30	0.54	0.74	053	0.28	0.19
0.05	0.44	0.54	0.81	1.03	0.84	0.61	0.54
0.00	0.61	0.74	1.03	1.27	1.11	0.90	0.85
-0.05	0.38	0.53	0.84	1.11	0.97	0.78	0.76
-0.10	0.11	0.28	0.61	0.90	0.78	0.62	0.61
-0.15	0.00	0.19	0.54	0.85	0.76	0.61	0.62

Figure S3.□Eff-PESs of 4-unit model of H-TTF at a) 293 K and b) 50 K and c) D-TTF at 270 K. In Figure S3(c), ΔE at (δ_{OH1}, δ_{OH2})=(-0.2, -0.2), (-0.2, 0.2), (0.2, 0.2), were 1.06, 0.68, 0.68 kcal/mol, respectively. Note that we confirmed the energy minima at the corner of Figure S3(c) by additionally exploring the outer region (δ_{OH} < –0.15, and δ_{OH} > 0.15).

Table S1. Summation of Mulliken charge in each H(Cat-EDT-TTF) subunit (SU) defined by Figure S2 and H-bonding three atoms [O…H…O] for each hydrogen coordinate (δ_{OH}). Used models were 1- and 3-unit model of H-TTF at 50 K.

		δ_{OH} (Å)					
		0.00	0.05	0.10	0.15	0.20	0.25
1-unit model	SU1	0.51	0.39	0.28	0.21	0.19	0.18
(a)	SU2	0.51	0.62	0.71	0.77	0.78	0.76
	H-bond	-1.02	-1.01	-1.00	-0.98	-0.96	-0.94
3-unit model	SU1	0.53	0.52	0.50	0.49	0.48	0.47
(b)	SU2	0.54	0.56	0.58	0.60	0.61	0.63
	SU3	0.54	0.53	0.53	0.52	0.52	0.51
	SU4	0.54	0.54	0.55	0.56	0.56	0.57
	SU5	0.54	0.52	0.50	0.48	0.46	0.44
	SU6	0.53	0.54	0.56	0.57	0.58	0.59
	H-bond 1	-1.07	-1.07	-1.07	-1.07	-1.07	-1.07
	H-bond 2	-1.09	-1.09	-1.08	-1.08	-1.08	-1.07
	H-bond 3	-1.07	-1.07	-1.07	-1.07	-1.07	-1.07

Table S2. Spin multiplicity of 1- and 3-unit model of H-TTF at 50 K. In 1-unit model, doublet state was the most stable regardless of δ_{OH}. Similarly, quartet state was the most stable in 3-unit model. We can expect almost the same energy barrier for doublet and quartet state in 3-unit model. However, spin contamination can be seen for doublet state. Thus, we assumed the spin multiplicity S=n+1, which can be expected to be most stable without spin contamination, for (H-TTF)$_n$ and (D-TTF)$_n$.

Models	δ_{OH}	Spin multiplicity	ΔE (kcal/mol)	$<S^2>_{calc}$	Energy barrier* (kcal/mol)
1-unit	0.00	2	0.00	0.7501	3.44
		4	61.57	3.7506	5.54
		6	—	—	—
	0.20	2	0.00	0.7501	
		4	59.46	3.7503	
		6	128.53	8.7506	
3-unit	0.00	2	0.01	0.8366	0.29
		4	0.00	3.7503	0.29
		6	64.22	8.7506	0.18
	0.10	2	0.01	0.8375	
		4	0.00	3.7503	
		6	64.34	8.7506	

*The Difference of energy between δ_{OH}=0.00 and off-centered position in the same spin multiplicity.

References

[1] Kreibich, T.; Gross, E. K. U. Multicomponent Density-Functional Theory for Electrons and Nuclei. *Phys. Rev. Lett.* **2001**, 86, 2984.

[2] Udagawa, T.; Tachikawa, M. H/D isotope effect on porphine and porphycene molecules with multicomponent hybrid density functional theory. *J. Chem. Phys.* **2006**, 125, 244105.

[3] Udagawa, T.; Ishimoto, T.; Tachikawa, M. Theoretical Study of H/D Isotope Effects on Nuclear Magnetic Shieldings Using an ab initio Multi-Component Molecular Orbital Method. *Molecules*, **2013**, 18, 5209.

[4] Udagawa, T.; Tsuneda T.; Tachikawa M. Electron-nucleus correlation functional for multicomponent density-functional theory. *Phis. Rev. A*. **2014**, 89, 052519.

[5] Tachikawa. M.; Mori, K.; Nakai, H.; Iguchi, K. An extension of ab initio molecular orbital theory to nuclear motion. *Chem. Phys. Lett.* **1998**, 290, 437.

[6] Kita, Y.; Udagawa, T.; Tachikawa, M. Nuclear quantum effect on molecular magnetic properties for low barrier hydrogen-bonded systems based on multicomponent density functional theory. *J. Chem. Phys.* **2006**, 125, 244105.

[7] Raugei, S.; Klein, M.L. Nuclear Quantum Effects and Hydrogen Bonding in Liquids. *J. Am. Chem. Soc.* **2003**, 125, 8992.

[8] Shiga, M.; Suzuki, K.; Tachikawa, M. Efficient ab initio path integral hybrid Monte Carlo based on the fourth-order Trotter expansion: application to fluoride ion-water cluster. *J. Chem. Phys.* **2010**, 132, 114104.

[9] Yoshikawa, T.; Sugawara, S.; Takayanagi, T.; Shiga, M.; Tachikawa, M. Theoretical study on the mechanism of double proton transfer in porphycene by path-integral molecular dynamics simultations. *Chem. Phys. Lett.* **2010**, 496, 14.

[10] Dračínský, M.; Hodgkinson, P. Effects of quantum nuclear delocalisation on NMR parameters from path integral molecular dynamics. *Chemistry* 1, **2014**.

[11] Sugimori, K.: Kawabe, H. Theoretical study of NMR chemical shift indeced by H/D isotope effect. *Int. J. Quantum Chem.* **2010**, 110, 2989.

[12] Stare, J.; Mavri, J. Numerical solving of the vibrational time-independent Schrödinger equation in one and two dimensions using the variational method. *Comput. Phys. Commun.* **2002**, 143, 222.

[13] Stare, J.; Balint-Kurti, G.G. Fourier grid Hamiltonian method for solving the vibrational Schrödinger equation in internal coodinates: theory and test applications. *J. Phys. Chem. A.* **2003**, 107, 7204.

[14] Golubev, N.S.; Melikova, S.M.; Shchepkin, D.; Shenderovich, I.G.; Tolstoy, P.M.; Denisov, G.S. Interpretation of Hydrogen/Deuterium Isotope Effects on NMR Chemical Shifts of [FHF]- Ion Based on Calculations of Nuclear Magnetic Shielding Tensor Surface. *Zeitschrift Für Phys. Chemie,* **2003**, 217, 1549.

[15] Auer, A. a.; Gauss, J.; Stanton, J.F. Quantitative prediction of gas-phase 13C nuclear magnetic shielding constants. *J. Chem. Phys.* **2003**, 118, 10407.

[16] Ruud, K.; Astrand, P.O.; Taylor, P.R. Zero-point vibrational effects on proton shieldings: Functional-group contributions from ab initio calculations. *J. Am. Chem. Soc.* **2001**, 123, 4826.

[17] Isono, T.; Kamo, H.; Ueda, A.; Takahashi, K.; Nakao, A.; Kumai, R.; Nakao, H.; Kobayashi, K.; Murakami, Y.; Mori, H. Hydrogen bond-promoted metallic state in a purely organic single-component conductor under pressure. *Nat. Commun.* **2013**, 4, 1344.

[18] Ueda, A.; Yamada, S.; Isono, T.; Kamo, H.; Nakao, A.; Kumai, R.; Nakao, H.; Murakami, Y.; Yamamoto, K.; Nishio, Y.; Mori, H. Hydrogen-Bond-Dynamics-Based Switching of Conductivity and Magnetism: A Phase Transition Caused by Deuterium and Electron Transfer in a Hydrogen-Bonded Purely Organic Conductor Crystal. *J. Am. Chem. Soc.* **2014**, 136, 12184-12192.